sciendo

Civil and Environmental Engineering
Vol. 16, Issue 1, 107-118, DOI: 10.2478/cee-2020-0011

# NUMERICAL ANALYSIS OF REINFORCED CONCRETE SLAB WITH SUBSOIL

Marie KOZIELOVA[1], Zuzana MARCALIKOVA[1,*], Pavlina MATECKOVA[1], Oldrich SUCHARDA[2]

[1] Department of Structures, Faculty of Civil Engineering, VSB - Technical University of Ostrava, Ludvíka Podéště 1875/17, 708 33 Ostrava-Poruba, Czech Republic.
[2] Department of Building Materials and Diagnostics of Structures, Faculty of Civil Engineering, VSB - Technical University of Ostrava, Ludvíka Podéště 1875/17, 708 33 Ostrava-Poruba, Czech Republic.
[*] corresponding author: zuzana.marcalikova@vsb.cz.

**Abstract**

The article deals with the interaction of a reinforced concrete slab with subsoil. The paper contains a non-linear analysis based on an experiment of reinforced concrete slabs with dimensions 2000 x 2000 mm and thickness 150 mm. A steel mesh with a diameter of 8/100 mm was used as reinforcement. The calculations and analysis are complemented by a comparison with EC2 design approaches. The research area combines the design of concrete structure and geotechnical tasks. The real behavior of the concrete structure with subsoil is considered for the analysis for advanced design. The selected computational approach of nonlinear analysis allows to capture the change of stiffness after the creation of cracks and modelling the shear punch failure of the slab - the collapse of the structure. The paper focuses on comparing the experiment with the numerical model in select loaded states for various input parameters of subsoil. Based on the experiment and numerical analysis the failure mechanism was determined. It was the punching of the slab. The calculations and the experiment verified that the critically controlled perimeter is at a distance of 1*d*. The effect of the modulus of elasticity on the slab punch mechanism was verified. In case of low modulus of subsoil, the load-bearing capacity of the slab is significantly reduced. The punching mechanism is influenced not only by the mechanical properties of the concrete but also by the properties of the subsoil. The performed parametric study also verified the influence of the size the nominal cover reinforcement depending on the modulus of elasticity of the subsoil. The deformation variant finite element method and a 3D computational model were used for numerical modelling. Nonlinear analysis was based on the Newton-Rapson method.

**Keywords:**

Concrete;
Numerical analysis;
Slab;
Subsoil.

## 1 Introduction

When designing a building structure, it is important to choose the appropriate foundation structure, which is suitable in terms of statics and cost. It is selected the type of the foundation mainly according to the type of geotechnical conditions. Typical flat foundation structures include foundation slabs, rafts, footing, where research is focused on this area. In designing and analysis foundation slabs, it is possible to apply a similar principle as during designing the floor structure. The typical mechanism of failure by punching [1] is very similar.

The very subject of dealing with the interaction of the foundation and the subsoil is called Soil Structure Interaction (SSI) by many researchers and is shown on Fig. 1. SSI connects three structural systems in total, that is the structure, the foundation and the subsoil, and there is a combination of two scientific fields, i.e. statics (the design and analysis of structure) [2, 3] and geotechnics (the analysis of the subsoil) [4-6]. SSI is an important part of various structural problems, particularly in the case of specific foundation conditions, very extreme loads [7] or dynamic analysis [8]. Due to these reasons, it is important to understand the mechanism of the interaction [9] and the choice of an appropriate computational model [10, 11]. Calculation using the slab equation and the Winkler model of subsoil is among typical analytical approaches to this problem in the form of differential equations:

$$D\nabla w(x,y) + kw(x,y) = q(x,y), \tag{1}$$

where *D* is the slab stiffness, *k* is the stiffness coefficient of the subsoil, *w* is the deflection and *q* is the applied load.

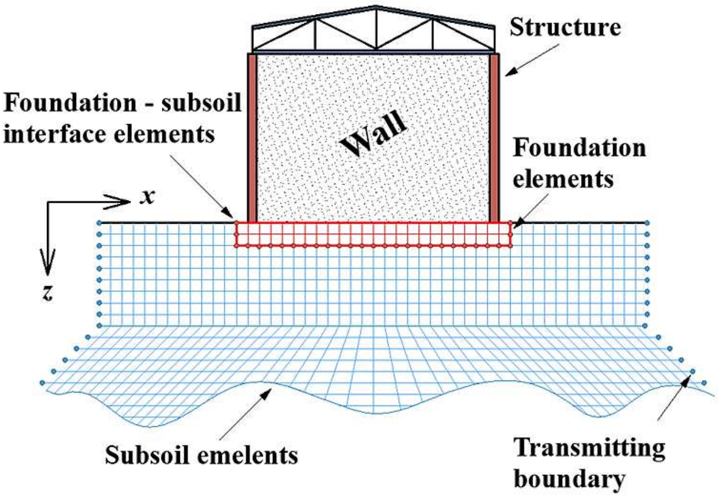


Fig. 1: SSI – Soil Structure Interaction.

This analytical approach is often suitable for the structural design, where the subsoil has to be homogenized into one stiffness constant on the basis of geotechnical investigation.

However, the problem solved is typically more complex and can be illustrated in the form of Fig. 2 and shows the SSI task (Soil - Structure Interaction). In the detailed SSI analysis, it is necessary to select the right parameters for the model, stiffness of subsoil and modelling the interaction between these two systems [6], [2]. It is also recommended to choose an approach to modelling the failure of concrete such in case of share and punching [12, 13]. In summary, this leads to the use of nonlinear analysis especially in the case, where the total bearing capacity is being measured. For numerical analysis, it is then possible to use the finite element method in combination with nonlinear analysis [14-16], which is currently the most used method. The finite element method [17] principle is based on the discretization of the computational model in a number of areas, where for the task at hand it is choosing an appropriate size of the modelled subsoil and input parameters for materials.

The finite element method [18] is based on solving systems of equations:

$$\mathbf{K} \cdot \mathbf{u} = \mathbf{F}, \tag{2}$$

where **K** is the stiffness matrix of the structure, **u** is a vector of unknown displacements and **F** is a vector of nodal loads. The finite element method can be modified for nonlinear analysis, where the calculation is divided into an incremental solution for the Newton-Raphson variant:

$$\mathbf{K(u)} \cdot \Delta\mathbf{u_i} = \Delta\mathbf{F_i}, \tag{3}$$

where **K(u)** is the stiffness matrix of the structure dependent on the displacement vector **u**, $\Delta\mathbf{u}_i$ is the deformation increment for the load step $\Delta\mathbf{F}_i$.

The use of nonlinear analysis alone makes it possible to perform sophisticated calculations and, in the case of reinforced concrete construction, to simulate failure and collapse mechanisms.

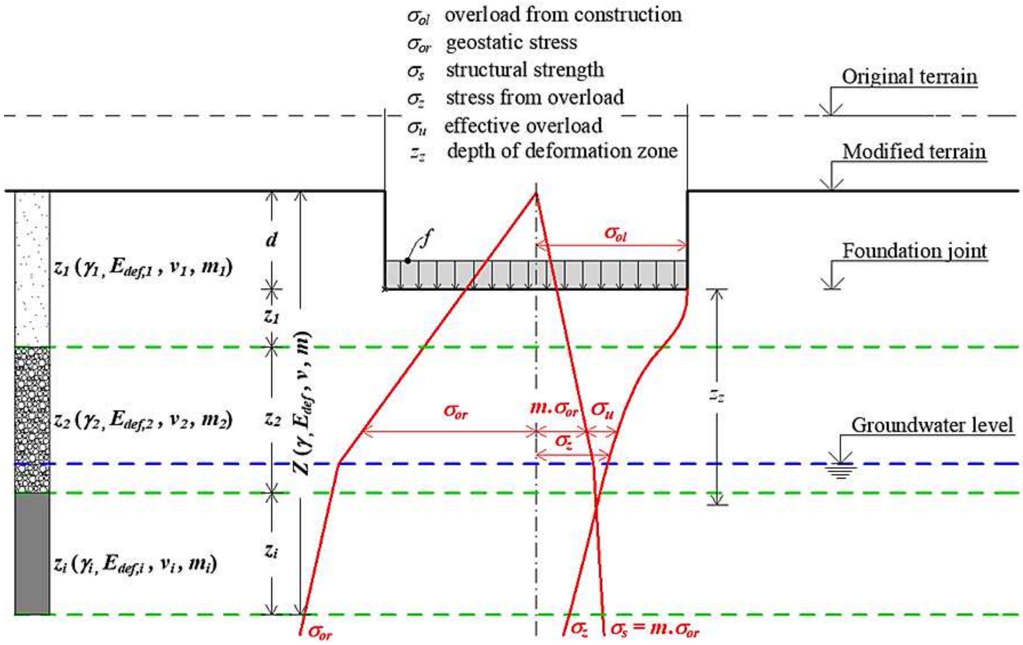


Fig. 2: Model for calculation of stress in foundation soil.

However, important sources of new knowledge include the implementation of experimental research into the structural behavior of SSI (maximum bearing capacity, shear reinforcement needs, shear capacity) [19-22], which are then needed for numerical modelling.

## 2 Punching failure of concrete slabs

Punching failure is a phenomenon which happens when a concentrated load is applied on a small area. Among typical structural elements, where there is shear punching failure, are for example concrete flat slabs or foundations under columns. These elements must be checked for according to the valid CSN EN 1992-1-1 standard [23]. Shear resistance should be checked at the face of the column and in the basic control perimeter $u_1$ at a distance of 2*d* from the face of the column (*d* - an effective depth of a cross-section, see Fig. 3). Checking control perimeter at distances less than 2*d* should be considered if the concentrated force resists high pressure, e.g. ground pressure on the foundation.

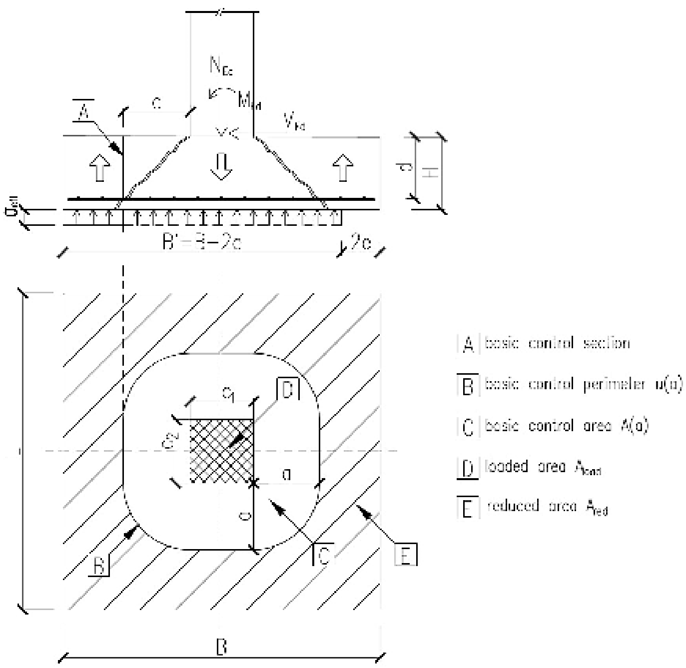


Fig. 3: Punching failure of column base.

The punching resistance of a column bases should be calculated according to the relation:

$$v_{Rd}(a) = max\begin{cases} C_{Rd,c} \cdot k \cdot (100 \cdot \rho \cdot f_{ck})^{\frac{1}{3}} \cdot \frac{2d}{a} \\ v_{min} \cdot \frac{2d}{a} \end{cases}. \tag{4}$$

Value $C_{Rd,c}$ = 0.18 /$\gamma_c$ where $\gamma_c$ = 1.5. Coefficient $k$ depends on the effective cross-section height $d$ in *mm* and expresses the influence of the cross-section height:

$$k = 1 + \sqrt{\frac{200}{d}} \leq 2{,}0\ . \tag{5}$$

Reinforcement ratio $\rho$ is defined by:

$$\rho = \sqrt{\rho_y \cdot \rho_z} \leq 0{,}02, \tag{6}$$

where $\rho_y$ and $\rho_z$ relate to the bonded tension reinforcement in *y*- and *z*- directions respectively. The values should be calculated as average values taking into account a slab width equal to the column width plus 3$d$ each side. Distance $a$ is the distance of the control perimeter under consideration from the column periphery. Characteristic strength of concrete $f_{ck}$ is in MPa. Value $v_{min}$ is expressed as:

$$v_{min} = 0.035 \cdot k^{\frac{3}{2}} \cdot f_{ck}^{\frac{1}{2}}\ . \tag{7}$$

If eccentric load is applied:

$$v_{Ed}(a) = \beta \frac{V_{Ed,red}(a)}{d \cdot u(a)}\ . \tag{8}$$

Coefficient $\beta$ expresses the influence of eccentric loading of the contact surface. Shear force $V_{Ed,red}$ is a shear force, which causes punching:

$$V_{Ed,red}(a) = V_{Ed} - \Delta V_{Ed}(a)\ , \tag{9}$$

where $V_{Ed}$ is the applied shear force and $\Delta V_{Ed}$ is the net upward force within the control perimeter considered i.e. upward pressure from soil minus self-weight of the base. Condition of bearing capacity:

$$v_{Rd,c}(a) \geq v_{Ed}(a)\ . \tag{10}$$

If the load-bearing condition is not met, then measures to increase the shear resistance must be taken. Suitable measures are: increase slab thickness/increase foundation depth, increase concrete quality, increase of bending reinforcement or shear reinforcement design. In the case of eccentric loading, a beta factor is taken into account in the calculation of the shear force, which takes into account the moments in the structural member.

## 3 Experiment

A reinforced concrete slab with dimensions of 2000 x 2000 mm and a thickness of 150 mm [24] was used for an experiment which provided data for numerical modelling. The scheme of the experiment is shown in Fig. 4. The slab was made of C35/45 concrete with Ø 8/100 mm steel reinforcement mesh, see Fig. 5. The nominal cover reinforcement for slab was 30 mm. The subsoil, which was classified as clay soil, was left under the testing equipment. The specialized testing equipment used is located at the Faculty of Civil Engineering, VSB - Technical University of Ostrava (Czech Republic).

The specialized testing equipment includes a steel frame, a hydraulic jack with capacity up to 1000 kN and a measuring centre with deformation sensors 16 sensors (as is from shown in Fig. 4 from 00 to 25) were used in the specific test, see Fig. 4. A load test was performed in 75 kN steps. A load was applied gradually at intervals of 30 minutes until the load-bearing capacity of the slab was reached.

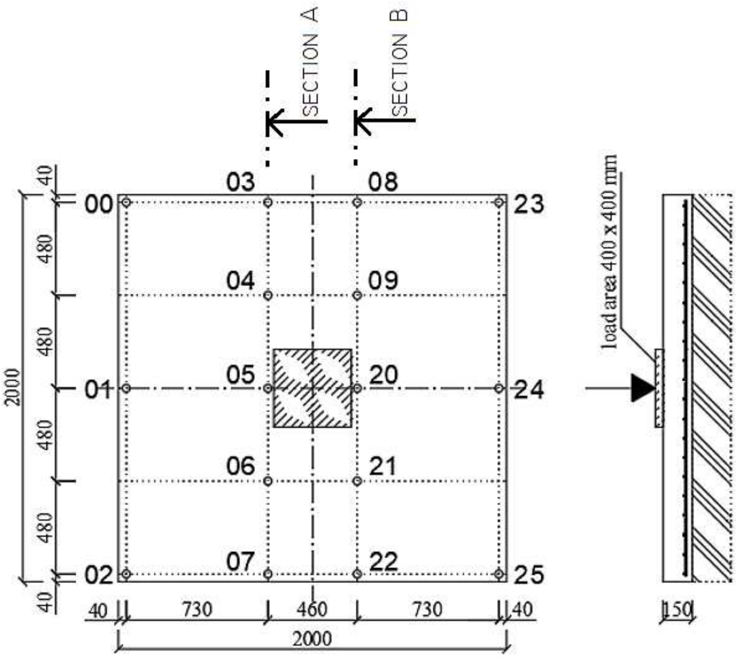


Fig. 4: The reinforcement concrete slab: scheme of the experiment.

Fig. 5: The reinforcement concrete slab (left), reinforcing of the slab (right).

The loading of the slab took place in load cycles. The experiment included two load cycles. The second load cycle is used to verify the effect of reduced bending stiffness of reinforced concrete weakened due to cracks and soil consolidation in the first load cycle, on deflection. Both load cycles included of load steps. The load step size was 75 kN/30 min. The last load step was 750 kN. The 300 kN, 450 kN and 750 kN loading steps were chosen for comparison of numerical modelling and experiment. The load step with a force of 300 kN corresponds to the closest calculated maximum force for bending moment. The maximum bending moment was calculated from the load of 285 kN. The comparison and the resulting deformation curves were evaluated for the cross-section corresponding to the sensors numbered 03 to 07 – section A, (see Fig. 6) and for the cross-section corresponding to the sensors numbered 08 to 22 – section B, (see Fig. 7). It can be seen Fig. 8 and 9 the detail of shear crack in section 1 a 3 after the experiment. During a load of 300 kN, very little deformation occurred, maximum 3 mm. At 750 kN, cracks were visible in the slab, but the slab remained compact. During the experiment punching failure did not occur and the reinforcement was not interrupted; only plastic deformations occurred.

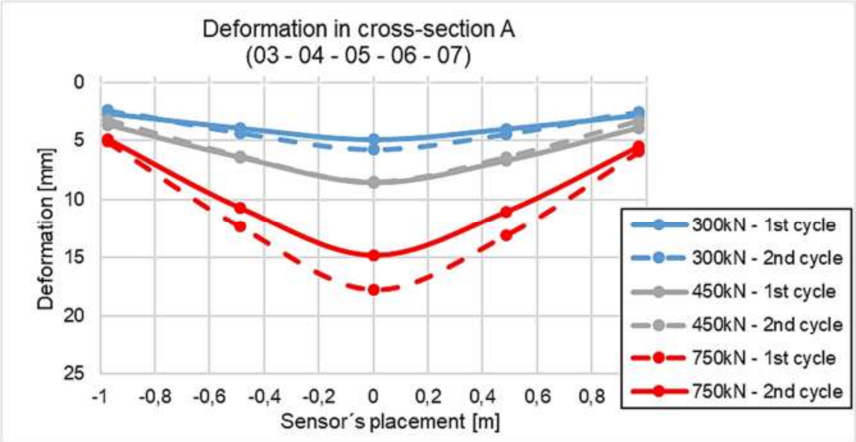


Fig. 6: Resulting deformation curves – section A.

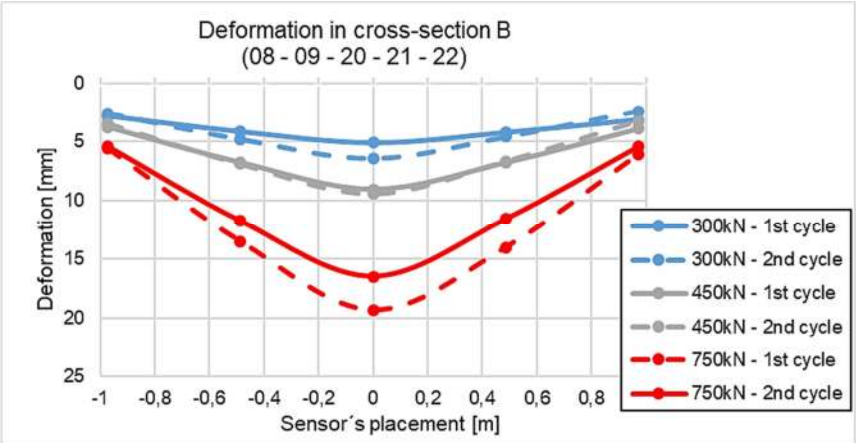


Fig. 7: Resulting deformation curves – section B.


Fig. 8: Detail of shear crack – section 1


Fig. 9: Detail of shear crack – section 3.

### 4 Numerical analysis

The primary aim of the numerical modelling was to determine the overall load-bearing capacity of the slab and to analyse its failure. Due to the specification of the analysis, 3D computational models were used, see Figs. 10 and 11. The calculation is based on a nonlinear analysis in the ATENA system [10]. Parameters are selected with respect to CEB-FIP Model Code 1990 [25] in the input parameter generator for material model Cementitious2. Parameters of concrete and reinforcement for numerical model are given in Table 1 and Table 2. The 3D computational model included a concrete slab, a steel support slab for loading and subsoil with a depth of 2 m. The finite element mesh has a regular shape. The detail of the finite element mesh is shown in Figs. 10 and 11. The ground plan size of the model was 6 x 6 m. In the case of the subsoil, a variant solution with a modulus of elasticity *E* 12.5, 17.5 and 22.5 MPa was used. The steel reinforcement was modelled by discrete 1D beams. The mean values of steel for input material parameters were used for calculation. The computational model also respects the modelling recommendations [11]. A contact interface is modelled between the slab and subsoil. The task was solved by the Newton-Raphson method. The load was applied by force in steps of 10 kN.

Table 1: Parameters of concrete for numerical model.

| | | |
|---|---|---|
| Modulus of elasticity | 34 | GPa |
| Poisson coefficient | 0.2 | - |
| Tensile strength | 3.2 | MPa |
| Compressive strength | 43 | MPa |
| Specific fracture energy | 80 | N/m |
| Rotation of cracks | fixed | |
| Max. aggregate size | 16 | |

Table 2: Parameters of reinforcement for numerical model.

| | | |
|---|---|---|
| Modulus of elasticity | 200 | GPa |
| Yield strength | 550 | Mpa |
| Tensile strength | 577.5 | MPa |
| Poisson coefficient | 0.2 | - |
| $\varepsilon_{lim}$ | 0.025 | - |
| $k$ | 1.05 | - |
| Safety format | mean | |
| Class of reinforcement | A | |

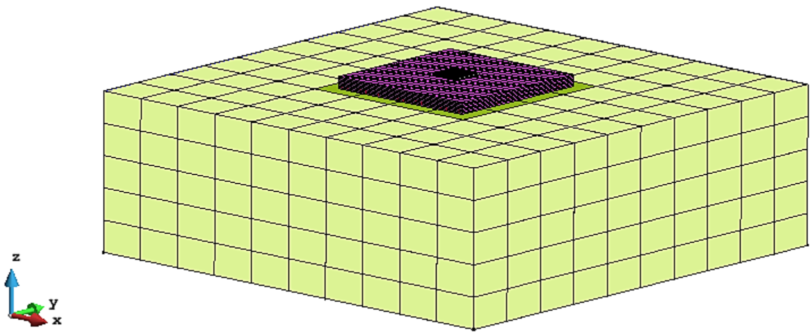

Fig. 10: 3D Computational model - mesh finite elements.

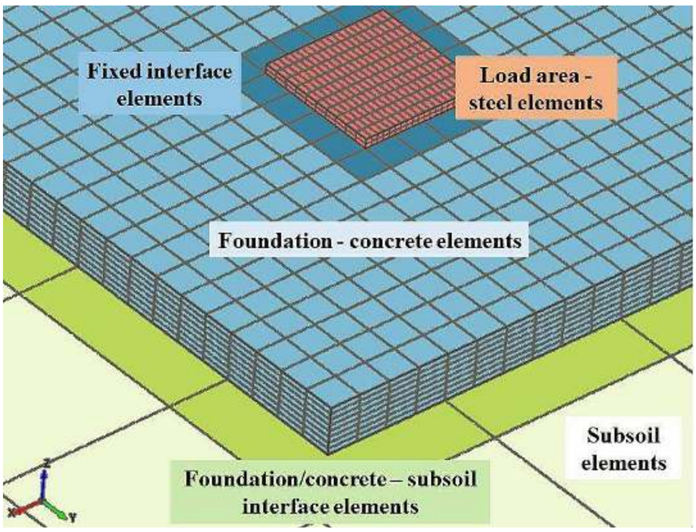

Fig. 11: Detailed scheme of 3D model.

Fig. 12 shows calculated stresses in reinforcement for load 450 kN and Fig. 13 shows cracks in the concrete slab. For a load of 300 kN, the normal stress in the reinforcement according to the linear calculation is 526 MPa. According to a calculation based on numerical models (non-linear calculations), the stress value was around 394 MPa, see Table 3. From this comparison, it is evident that the action of soil below the foundation reduces the stress in the reinforcement. Fig. 14 and Fig. 15 show the normal stress $\sigma_x$ and $\sigma_z$ of subsoil for a load of 450 kN. The normal stress $\sigma_z$ is significantly greater than the normal stress $\sigma_x$.

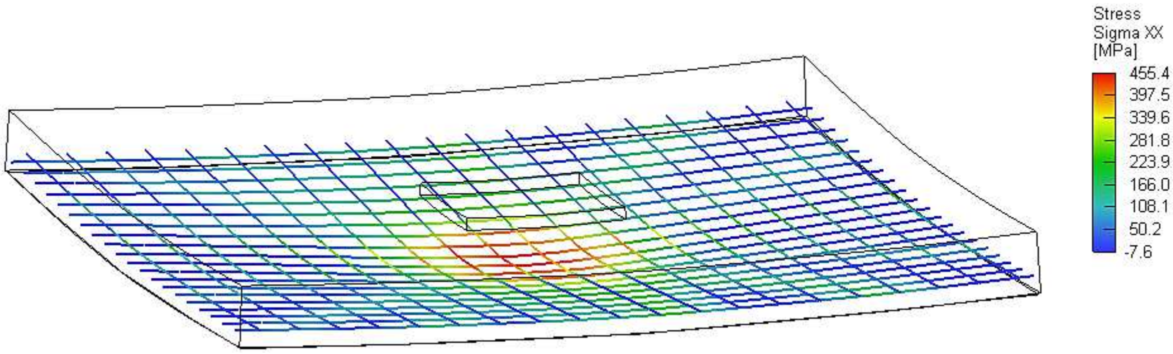


Fig. 12: Normal stresses $\sigma_x$ in steel reinforcement - Load 450 kN.

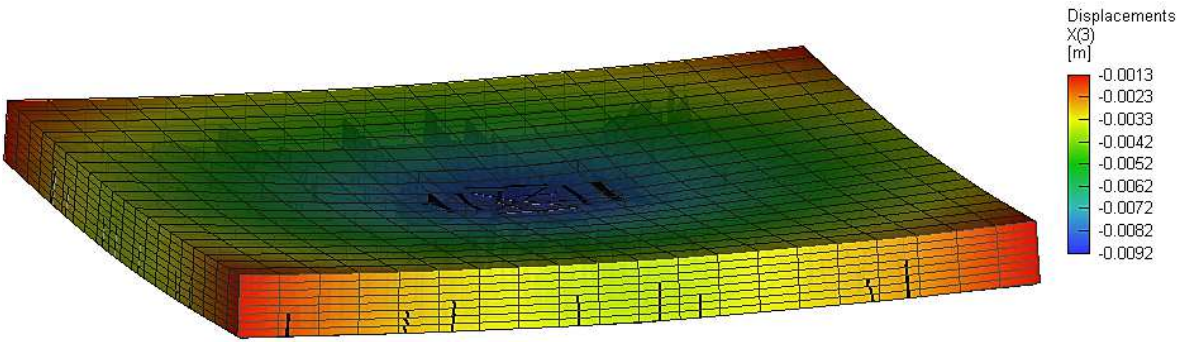


Fig. 13: Deformations of concrete slab with crack (min.0.1 mm) - Load 450 kN.

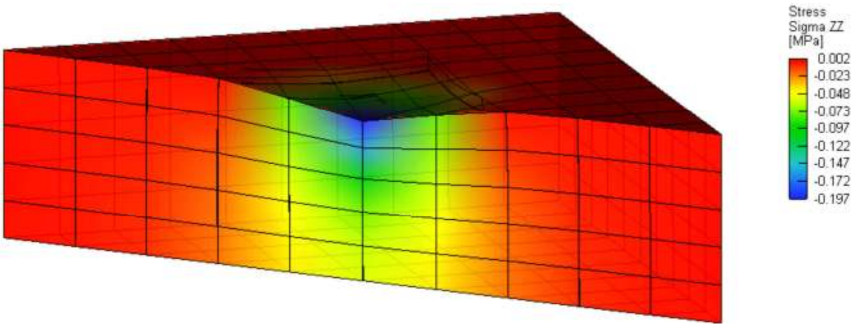


Fig. 14: Normal $\sigma_z$ - Load 450 kN.

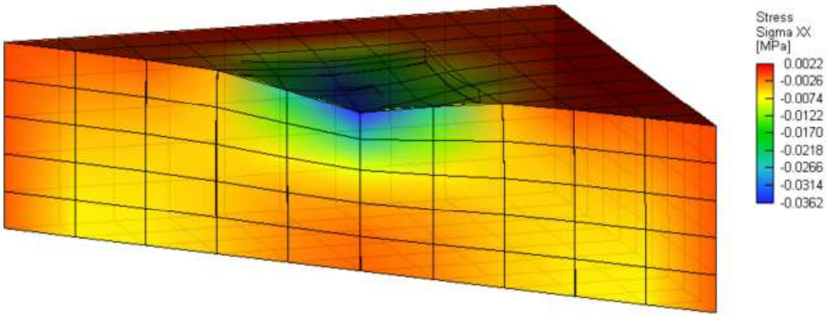


Fig. 15: Normal $\sigma_x$ - Load 450 kN.

Table 3: Comparison of resulting values of deformations.

| **Load [kN]** | **Experiment [mm]** | | **Computational model [mm]** | **$\sigma_x$ in the reinforcement [MPa]** |
|---|---|---|---|---|
| | Section A | Section B | | |
| 300 | 4.9 – 5.8 | 5.1 – 6.4 | 5.3 | 394 |
| 450 | 8.5 – 8.6 | 9.1 – 9.4 | 9.0 | 455 |
| 750 | 14.8 – 17.8 | 16.5 – 19.3 | 17.1 | 553 |

## 5 Results and discussions

The performed calculations of the slab in interaction with the subsoil were in a variant solution. The results of the calculations showed that the overall bearing capacity is significantly influenced by the parameters of subsoil and reinforcement. Two calculation variants were chosen to verify the influence of the nominal cover on the total load-bearing capacity. In the Table 4 is comparison load-bearing capacity in the dependency on the effective high of a cross-section for the nominal cover of reinforcement 15 and 30 mm. The effective high of a cross-section is 127 mm for the nominal cover 15 mm and 112 mm for the nominal cover 30 mm. Resulting values in Table 4 were determined according to CSN EN 1992-1-1 [23].

Table 4: Resulting values of load-bearing capacity for punching [kN].

| **Control perimeter at a distance *d*** | **Nominal cover 15 mm** | **Nominal cover 30 mm** |
|---|---|---|
| 0.5 *d* | 1234 | 1104 |
| 1 *d* | 769 | 673 |
| 1.5 *d* | 664 | 563 |
| 2 *d* | 537 | 457 |

The reinforced concrete slab was pushed into the subsoil during the experiment. The total load-bearing capacity of the reinforced concrete slab was about 750 kN. For non-linear analysis, the test result was 770 kN and according to the calculation was 769 kN and 673 kN. Once the tensile strength of the concrete is reached in the middle of the underside of the slab, cracks and lifting of the slab edges occur. Cracking spread from the centre to the edges of the slab, in one to two dominant vertical crack lines. The concrete slab remained whole during and after the test. Fig. 16 shows a computer model with cracks and a concrete slab after a load test.

The results of the experiment and numerical calculations are best captured by the calculation for modulus of elasticity of the subsoil of 22.5 MPa. This value is typical of the test soil in the experiment.

The conformity of the calculated deformations can be considered good for the overall computation model The greatest differences were particularly in the vicinity of the loading steel plate, where there was a high concentration of the tension in the concrete and the subsoil. Resulting values in Table 5 were obtained to the numerical modelling. The values for the condition of failure evaluation of the calculation are given in brackets. The convergence criterion (residual error) was assumed to be up to 5 % in the calculation. Exceeding the limit value was being evaluated as fatal failure to slab for evaluation.

Table 5: Resulting values of load-bearing capacity for punching [kN], deformation [mm], convergence criterion [%] – numerical modelling.

| **Modulus of elasticity [MPa]** | **Nominal cover 15 mm** | **Nominal cover 30 mm** |
|---|---|---|
| 12.5 | 550/17.4 (5.1) | 510/16.7 (5.1) |
| 17.5 | 670/17.3 (5.2) | 630/16.5 (5.1) |
| 22.5 | 770/16.8 (5.1) | 700/15.3 (5.9) |

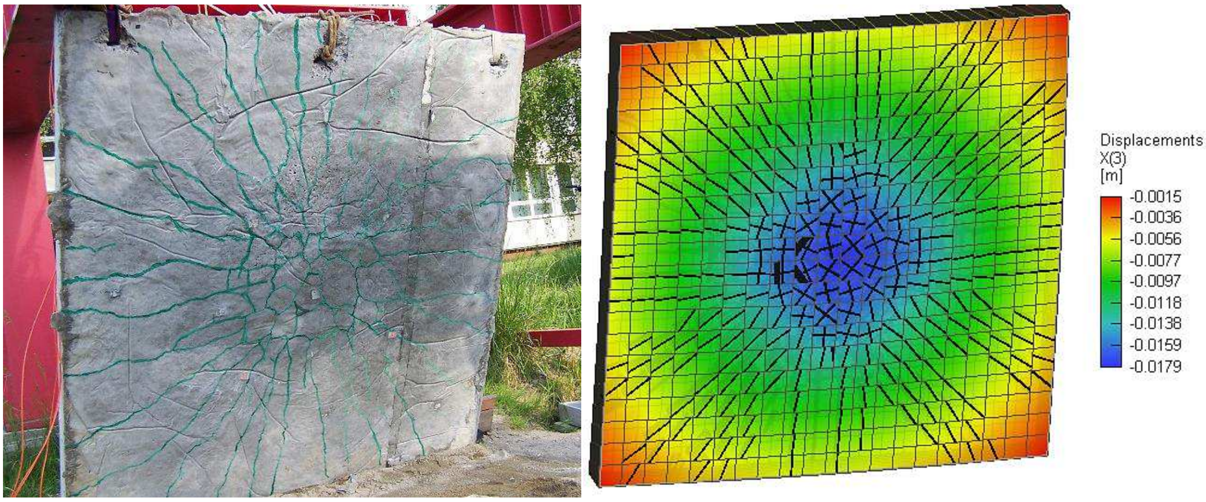


Fig. 16: Comparison of experimental test and numerical modelling of concrete slab with crack.

Comparison of experiment and performed non-linear analyses is shown in load displacement diagrams in Fig. 17. Calculations are set for a different modulus of subsoil and for the nominal cover of 30 mm. The graph shows influence of subsoil stiffness, which increases especially in cases of higher load. The graph shows the average slab deformations for sensors 05 and 20 from the experiment.

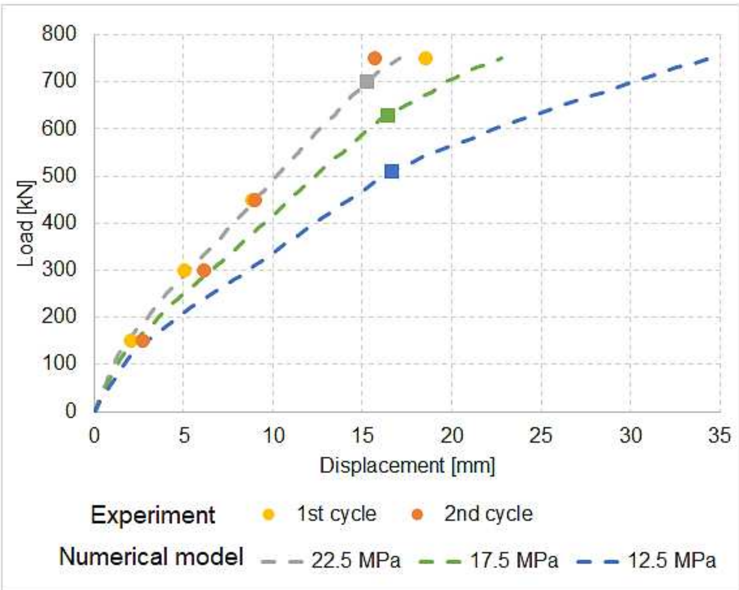


Fig. 17: LD diagrams - comparison of experimental test and numerical modelling of concrete slab.

## 6 Conclusion

The article deals with the modelling of the interaction of reinforcement slabs with subsoil and nonlinear analysis. The differences in resulting deformations in calculations and the experiment can be considered as acceptable for modulus of elasticity subsoil 22.5 MPa, because the results from experiment and from the computer model are in good conformity. Numerical calculations show, that cracks may form on the bottom side of the slab. From experimental and numerical calculations, it is obvious that the crack width increases with increase load. The concrete slab remained compact during and after the test (after achieve load 750 kN). The influence of subsoil stiffness increases with increasing damage to the reinforced concrete slab and load. With greater load, the reinforcement plasticized gradually near the applied load. Based on the performed calculations, it can be stated that the use of nonlinear analysis enables a detailed understanding of the mechanism of the collapse of the reinforced concrete slab in the interaction with subsoil and determine the influence of the input parameters of subsoil.

**Acknowledgments**

The work was supported by the means of conceptual development of science, research and innovation assigned to VŠB-TUO by the Ministry of Education, Youth and Sports of the Czech Republic.

**References**

[1] SIBURG, C. - HEGGER, J.: Experimental investigations on the punching behaviour of reinforced concrete footings with structural dimensions. Structural Concrete, Vol. 15, Iss. 3, 2014, DOI:10.1002/suco.201300083.
[2] TOMASOVICOVA, D. – JENDZELOVSKY, N.: Stiffness Analysis of the Subsoil under Industrial Floor. Procedia Engineering, Vol. 190, 2017, pp. 365-370, DOI:10.1016/j.proeng.2017.05.350.
[3] TOMASOVICOVA, D. - JENDZELOVSKY, N. - MARTON, P.: Damage analysis of the industrial floor in the storage hall. International Multidisciplinary Scientific GeoConference Surveying Geology and Mining Ecology Management, SGEM, Vol. 17, Iss. 12, 2017, pp. 191-198, DOI: 10.5593/sgem2017/12/S02.025.
[4] HRUBESOVA, E. - MOHYLA, M. - LAHUTA, H. - BUI, T.Q. - NGUYEN, P.D.: Experimental analysis of stresses in subsoil below a rectangular fiber concrete slab. Sustainability (Switzerland), Vol. 10, Iss. 7, art. no. 2216, 2018.
[5] PAZDERA, L. - CAJKA, R. - L. TOPOLÁŘ, - MATECKOVA, P. – BILEK, V. - SUCHARDA, O. Measurement and Utilization of Acoustic Emission for the Analysis and Monitoring of Concrete Slabs on the Subsoil. Periodica Polytechnica Civil Engineering, Vol. 63, Iss. 2, 2019, pp. 608-620, DOI:10.3311/PPci.12695.
[6] SUCHARDA, O. - SMIRAKOVA, M. - VASKOVA, J. - MATECKOVA, P.- KUBOSEK, J. - CAJKA, R.: Punching Shear Failure of Concrete Ground Supported Slab, International Journal of Concrete Structures and Materials, Vol. 12, Iss. 1, art. no. 36, 2018, DOI:10.1186/s40069-018-0263-6.
[7] KRÁLIK, J.: Probabilistic safety assessment of the design of tall buildings under the extreme load, AIP Conference Proceedings, 1738, art. no. 480088, 2016, DOI:10.1063/1.4952324.
[8] KOTRASOVA, K. - KORMANIKOVA, E. Dynamic analysis of liquid storage tanks. AIP Conference Proceedings, 1863, art. no. 260005, 2017, DOI:10.1063/1.4992419.
[9] SUCHARDA, O. - BILEK, V. - SMIRAKOVA, M. - KUBOSEK J. - CAJKA, R.: Comparative Evaluation of Mechanical Properties of Fibre Reinforced Concrete and Approach to Modelling of Bearing Capacity Ground Slab, Periodica Polytechnica Civil Engineering, Vol. 61, No. 4, 2017, DOI:10.3311/PPci.10688.
[10] CERVENKA, V. - JENDELE L. – CERVENKA, J.: ATENA Program documentation - Part 1: Theory. Cervenka Consulting. Pratur. 2016.
[11] SUCHARDA O. - KONECNY, P.: Recommendation for the modelling of 3D non-linear analysis of RC beam tests. Computers and Concrete, Vol. 21, Iss. 1, 2018, pp. 11-20, DOI:10.12989/cac.2018.21.1.011.
[12] AUGUSTIN, T. - FILLO, L. - HALVONIK J. - MARCIS, M.: Punching resistance of flat slabs with openings - experimental investigation, Solid State Phenomena, Vol. 272, 2018, pp. 41-46.
[13] VIDA, R. - HALVONIK, J.: Shear assessment of concrete bridge deck slabs, Key Engineering Materials vol. 738, 2017, pp. 110-119, DOI:10.4028/www.scientific.net/KEM.738.110.
[14] SUCHARDA, O. - BROZOVSKY, J. - MIKOLASEK, D.: Numerical modelling and bearing capacity of reinforced concrete beams, Key Engineering Materials, Vol. 577-578, 2014, pp. 281-284, DOI:10.4028/www.scientific.net/KEM.577-578.281.
[15] SUCHARDA, O. – KUBOSEK, J.: Modelling and analysis of reinforced concrete beams, Key Engineering Materials, Vol. 662, 2015, pp. 81-84, DOI:10.4028/www.scientific.net/KEM.662.81.
[16] WIECZOREK, B.: Numerical Model of the Load-Bearing Capacity of the Bottom Reinforcement Bars Passing over the Column, Procedia Engineering, Vol. 190, 2017, pp. 660-667, DOI:10.1016/j.proeng.2017.05.394.
[17] ZIENKIEWICZ, O.C. - TAYLOR, R.L.: The Finite Element Method, Fifth edition. Butterworth-Heinemann. Oxford, 2000.
[18] HOSTETTER, G. - MANG H.A.: Computational Mechanics of Reinforced Concrete Structures. Braunschweig/Wiesbaden: Vieweg-Verlag, 1995, 366 p.
[19] HEGGER, J. - RICKER, M. - ULKE, B. - ZIEGLER, M.: Investigations on the punching behaviour of reinforced concrete footings. Engineering Structures, Vol. 29, 2007, pp. 2233–2241, DOI:10.1016/j.engstruct.2006.11.012.
[20] HEGGER, J. - SHERIF, G.A. - RICKER, M.: Experimental investigations on punching behavior of reinforced concrete footings. ACI Structural Journal, Vol. 103, 2006, pp. 604–613.

[21] HOANG, L. C. - POP, A.: Punching shear capacity of reinforced concrete slabs with headed shear studs. Magazine of Concrete Research, Vol. 68, Iss. (3), 2016, pp. 118–126.
[22] HALVONIK, J. - FILLO, L.: The maximum punching shear resistance of flat slabs. Procedia Engineering, Vol. 65, 2013, pp. 376–381.
[23] EN 1992-1-1 (2004) (English): Eurocode 2: Design of concrete structures - Part 1-1: General rules and rules for buildings.
[24] BUCHTA, V. – JANULIKOVA, M. - FOJTIK, R.: Experimental Tests of Reinforced Concrete Foundation Slab. Procedia Engineering, Vol. 114, 2015, pp. 530-537, DOI:10.1016/j.proeng.2015.08.102.
[25] CEB-FIP Model Code 1990, First Draft, Comittee Euro-International du Beton, Bulletin d'information No. 195, 196, Mars.